New

Wind Library
File under
Fujita

Institute for Disaster Research
Texas Tech University
Post Office Box 4089
Lubbock, Texas 79409

Effects of the April 17, 1978 Tornado on the Grand Gulf Cooling Tower

P A R T II

(Report of Task B)

by
T. Theodore Fujita
Professor of Meteorology

Prepared for

Raths, Raths & Johnson, Inc.
907 North Elm Street
Hinsdale, Illinois 60521

January 31, 1979

Filed as SMRP 162 - II

Effects of the April 17, 1978 Tornado on the Grand Gulf Cooling Tower

P A R T II

(Report of Task B)

1. INTRODUCTION AND TERMINOLOGY

The objective of Task B is to determine the static pressure of the inner and outer surfaces of the tower shell at five different times: -4 seconds, -2 seconds, 0 second, +2 seconds, and +4 seconds. The time of 0 second is the estimated moment when the tower crane impacted on the tower shell.

Engineering and meteorological terms on tornado and high-wind effects are often different and confusing. For the purpose of clarifying the key terms, a glossary is presented in this section.

AERODYNAMIC PRESSURE, $P_A = C_p \Pi$

Pressure exerted by a disturbed flow upon the surface of a structure.

APPARENT INSIDE PRESSURE, P'_{in}

Hypothetical static pressure at the inner surface of the shell. This pressure is computed as the product of the edge-effect function and the apparent outside pressure.

APPARENT OUTSIDE PRESSURE, P'_{out}

Hypothetical static pressure at the outer surface of the shell computed by subtracting the mean inside pressure from the outside pressure which does not include the edge-effect.

DIFFERENTIAL PRESSURE, $\Delta P = P_{out} - P_{in} = P'_{out} - P'_{in}$

Pressure difference between inner and outer walls of a structure. Positive differential pressure causes the inward push, while the negative differential pressure causes the outward suction of the wall.

EDGE-EFFECT FUNCTION, $F(\Delta H)$

Non-dimensional function which decreases with the vertical distance from the tower edges, either top or base. This function is used for equalizing the static pressure at the edge.

INSIDE PRESSURE, P_{in}

Static pressure at the inner surface of a structure under the influence of an airflow and vortex pressure.

OUTSIDE PRESSURE, P_{out}

Static pressure at the outer surface of a structure under the influence of an airflow and vortex pressure.

PRESSURE COEFFICIENT, C_p

Non-dimensional quantity expressing the ratio, aerodynamic pressure divided by the stagnation pressure, at a given point on the shell surface.

STAGNATION PRESSURE, $\Pi = \frac{1}{2}\rho V_\beta^2$

Aerodynamic pressure induced when the undisturbed flow is to become stagnant at the shell surface.

STATIC PRESSURE, $P_s = P_v + P_A$

Total pressure induced by both tornado vortex and its airflow obstructed by a structure.

UNDISTURBED FLOW ANGLE, β

Direction of undisturbed flow velocity at the shell surface measured from the direction toward the center of the tower. Clockwise direction is positive.

UNDISTURBED FLOW SPEED, V_p

Speed of an airflow at the shell surface before perturbations are introduced by the cooling tower.

VORTEX PRESSURE, P_v

Negative pressure which provides the gradient force to maintain the airflow of an undisturbed tornado vortex.

2. PRESSURE DISTRIBUTION UNDER STRAIGHT-LINE WIND

The pressure coefficient at the outer surface of the shell of a cooling tower can be computed based on "Static and Dynamic Wind Effects on Cooling Tower Shells" by Hans-Juergen Niemann (ASCE Preprint 3031, October 1977).

The pressure coefficient, C_p , is extremely complicated. Niemann's Figures 2a through 2d indicate, however, that C_p can be expressed as a function of three parameters:

β , the undisturbed flow angle (see Figure 1),

k/a , the surface roughness. $k/a = 3.34 \times 10^{-2}$ for this case, and

ΔH , the vertical distance from the top (or base) of the shell. The ΔH dependence of the pressure coefficient is a result of the equalizing effects of the pressure on both sides of the cooling tower shell.

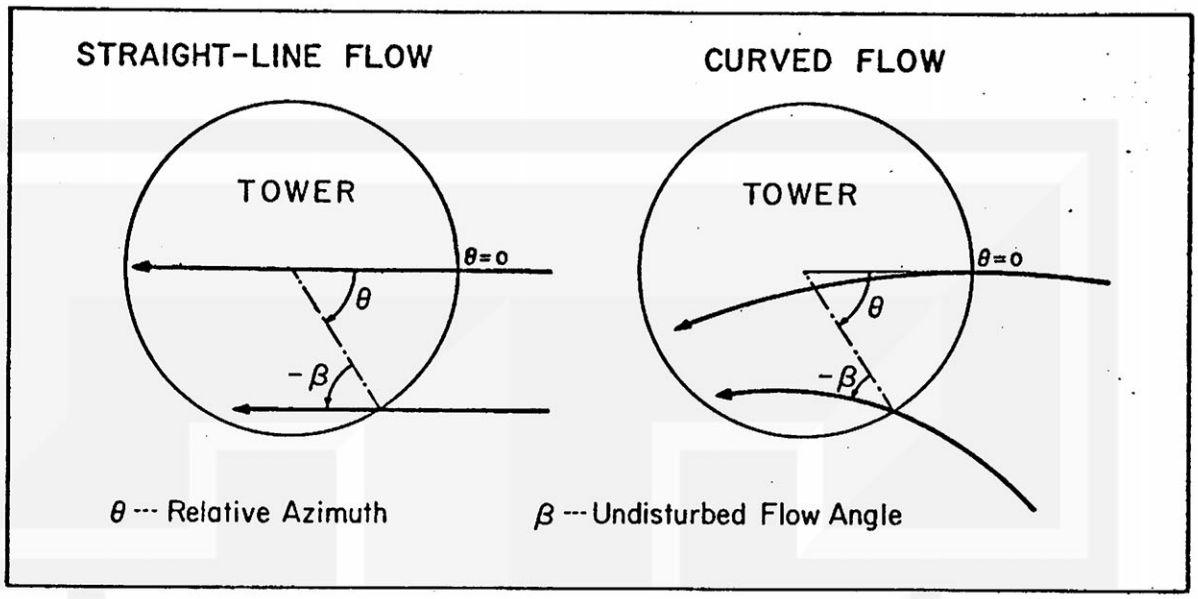

Figure 1. Definition of undisturbed flow angle applicable to straight-line flow (SLF) and curved flow.

First, we assume that C_p varies only with k/a and β to obtain Figure 2 and Table 1. A correction to the ΔH dependence will be performed later. Under this assumption, we compute the aerodynamic pressure outside the shell from

$$P_A = C_p \tfrac{1}{2} \rho V_\beta^2 \qquad (1)$$

where V_β denotes undisturbed flow speed.

Table 1. Flow angle, β given as a function of pressure coefficient C_p.

					Pressure Coefficient								
+1.0	+0.8	+0.6	+0.4	+0.2	0.0	-0.2	-0.4	-0.6	-0.8	-1.0	-0.8	-0.6	-0.5
0°	16	25	31	36	40	44	48	53	58	70	80	88	100
360°	344	335	329	324	320	316	312	307	302	290	280	272	260

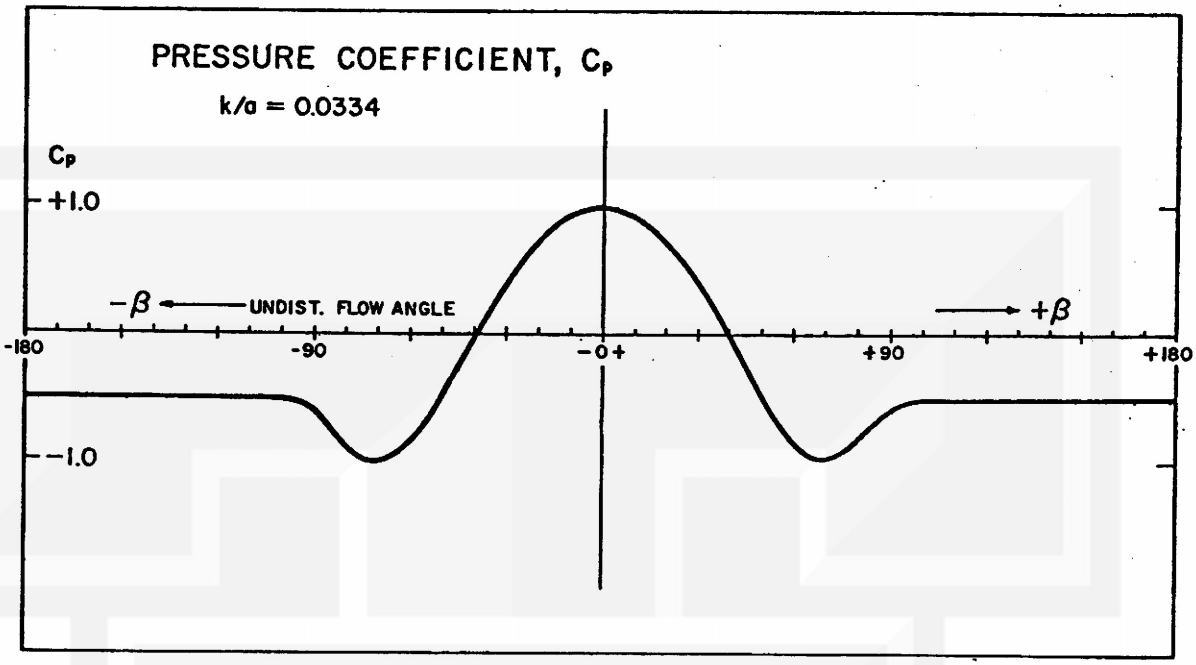

Figure 2. Pressure coefficient from Niemann (1977) plotted as a function of undisturbed flow angle.

Figure 3 shows an example of the pressure field around the Grand Gulf cooling tower when V_β is assumed to be 90 mph. The stagnation pressure corresponding to this wind speed is 14 centi-psi (cpsi) when the density of air is 0.002 g/cm^3 (see Table 2).

The mean aerodynamic pressure "inside the shell" is assumed to be the mean pressure averaged over the entire circumference at the top and at the base of the shell. This pressure is written as

$$\bar{P}_{in} = \frac{1}{720^\circ}\int_0^{360^\circ}(P_{base} + P_{top})\, d\theta \qquad (2)$$

Table 2. Windspeeds computed as a function of stagnation pressure, $\frac{1}{2}\rho V_\beta^2$. ρ is assumed to be 1.2×10^{-3} g/cm^3. Π ... stagnation pressure in centi-psi (cpsi).

Π	V_β	Π	V_β	Π	V_β
0 cpsi	0 mph	8 cpsi	68 mph	20 cpsi	107 mph
1	24	9	72	25	120
2	34	10	76	30	131
3	42	11	80	35	142
4	48	12	83	40	151
5	54	13	87	45	161
6	59	14	90	50	170
7	63	15	93	55	178

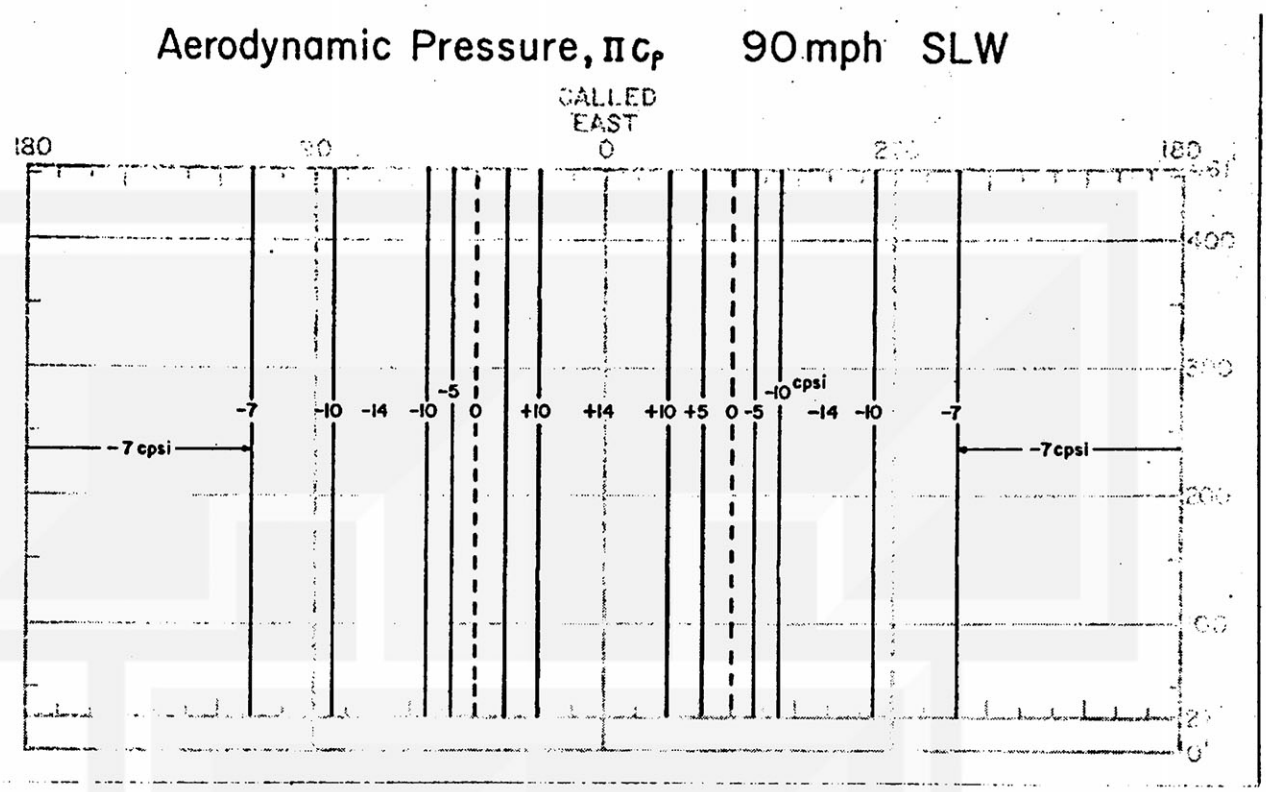

Figure 3. Aerodynamic pressure outside the tower shell under the influence of a 90 mph straight-line wind.

where $\bar{P}_{in}$ denotes the mean inside pressure; P_{base} and P_{top}, those at the base and the top, respectively; and θ, the tower azimuth. The mean inside pressure, thus computed from Figure 3 is

$$\bar{P}_{in} = -0.302 \times 14 = -4.2 \text{ cpsi} \quad (3)$$

This mean pressure inside the tower is valid as long as the internal air motion, including the updraft, remains relatively small, say, less than 30 mph, which induces the aerodynamic pressure of 2 cpsi.

The equalization processes of the pressure near the top and the base of the tower induce a sub-tower scale flow described schematically in Figure 4. The effect of the flow on the static pressure is to reduce the pressure difference on both sides of the shell near the top or the base of the tower. Since the atmosphere cannot maintain a pressure discontinuity unless it is separated by a solid wall or shell, the static pressure on both sides of the shell, only a few inches above the top or below the base, will have to be equal. Infinite pressure gradient does not exist in the free atmosphere.

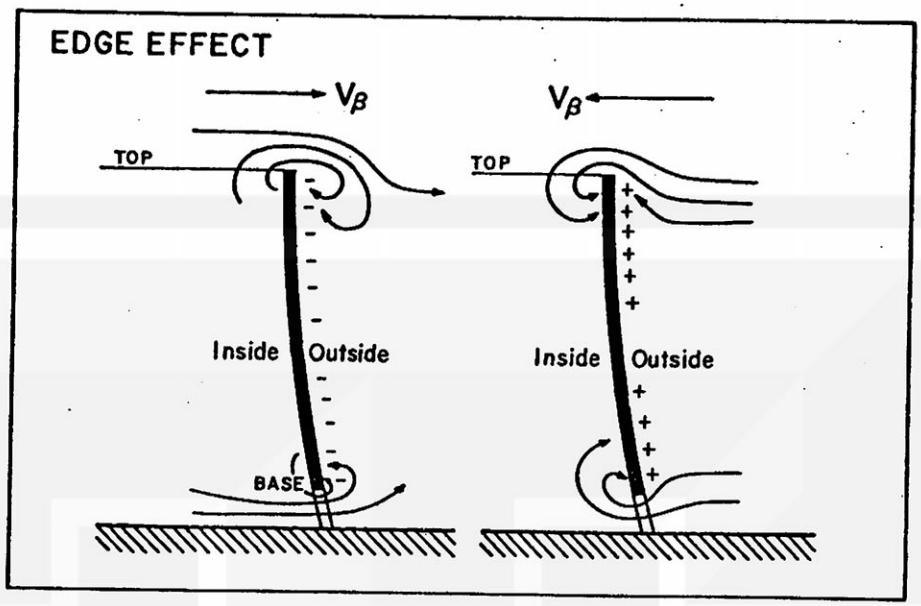

Figure 4. Edge effect which induces a sub-tower scale flow which equalizes the pressure on both sides of the shell.

Niemann's pressure coefficient in his Figure 2a implies that the equalization flow extends to about one-tenth of the tower height.

Expressing the vertical distance, ΔH in ft from either the top or the base of the tower, we write

$$P_{in} = \overline{P}_{in} + (P_{out} - \overline{P}_{in})F(\Delta H) \quad (4)$$

$$\text{where } F(\Delta H) = e^{-0.05\Delta H} \quad (5)$$

may be called the edge-effect function which decreases exponentially from the top downward or from the base upward. This function reaches 0.1 at ΔH between 40 and 50 ft (see Table 3).

Table 3. Numerical values of the edge-effect function computed as a function of ΔH, the vertical distance from the top or base edge of the cooling tower.

ΔH	$f(\Delta H)$	ΔH	$f(\Delta H)$	ΔH	$f(\Delta H)$	ΔH	$f(\Delta H)$
0 ft	1.000	5 ft	0.779	10 ft	0.606	60 ft	0.050
1	0.951	6	0.741	20	0.368	70	0.030
2	0.905	7	0.705	30	0.223	80	0.018
3	0.861	8	0.670	40	0.135	90	0.011
4	0.819	9	0.638	50	0.082	100	0.007

Differential pressure is defined as the difference in the static pressure

$$\Delta P = P_{out} - P_{in} \tag{6}$$

where "out" and "in" denote outside and inside the shell, respectively.

Theoretically, both P_{out} and P_{in} must include the ΔH dependent edge-effect function in order to equalize the pressure. What we need ultimately is, however, the differential pressure, ΔP, that can be computed quickly by introducing two new types of pressure identified as

P'_{in} , Apparent inside pressure, and

P'_{out} , Apparent outside pressure.

Introduction of these two types of pressures permit us to accelerate computations of the differential pressure in Eq. (6).

Now we combine Eq. (6) with Eq. (4) to write

$$\Delta P = (P_{out} - \bar{P}_{in}) - (P_{out} - \bar{P}_{in})F(\Delta H). \tag{7}$$

The two terms on the right side of this equation are called the "apparent outside pressure"

$$P'_{out} = P_{out} - \bar{P}_{in} \tag{8}$$

and the "apparent inside pressure"

$$P'_{in} = (P_{out} - \bar{P}_{in})F(\Delta H)$$

$$= P'_{out} \; F(\Delta H) \tag{9}$$

It should be noted that the apparent outside pressure is free from the edge-effect function while the apparent inside pressure is computed as the product of the apparent outside pressure and the edge-effect function.

Obviously, we are able to compute the differential pressure, ΔP, from

$$\Delta P = P'_{out} - P'_{in} \tag{10}$$

which is much simpler in computing the differential pressure from

$$\Delta P = P_{out}\left[1 - F(\Delta H)\right] - \bar{P}_{in}\left[1 - F(\Delta H)\right] \tag{11}$$

because, both terms on the right side include the edge-effect function.

Figure 3, showing the isobars (lines of equal pressures) computed from Eq. (1), is now converted into

$$P'_{out} = P_{out} - \bar{P}_{in} \tag{12}$$

where $P_{out} = P_A$ in Eq. (1). The field of apparent outside pressure from Eq. (12) is shown in Figure 5.

The apparent inside pressure from Eq. (9) is presented in Figure 6 with isobars drawn for every 5 cpsi interval. The differential pressure acting upon the shell can be obtained simply by computing the the difference in the pressure fields in Figures 5 and 6.

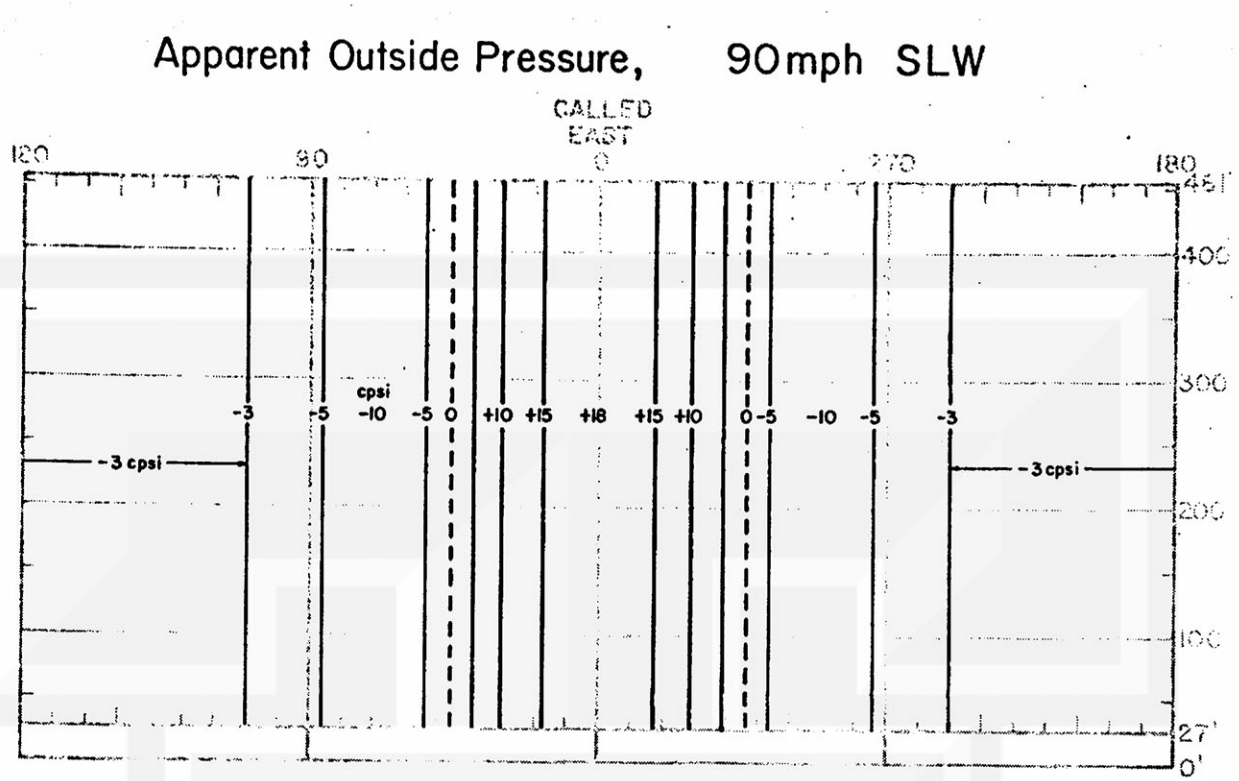

Figure 5. Apparent outside pressure induced by a 90 mph straight-line wind.

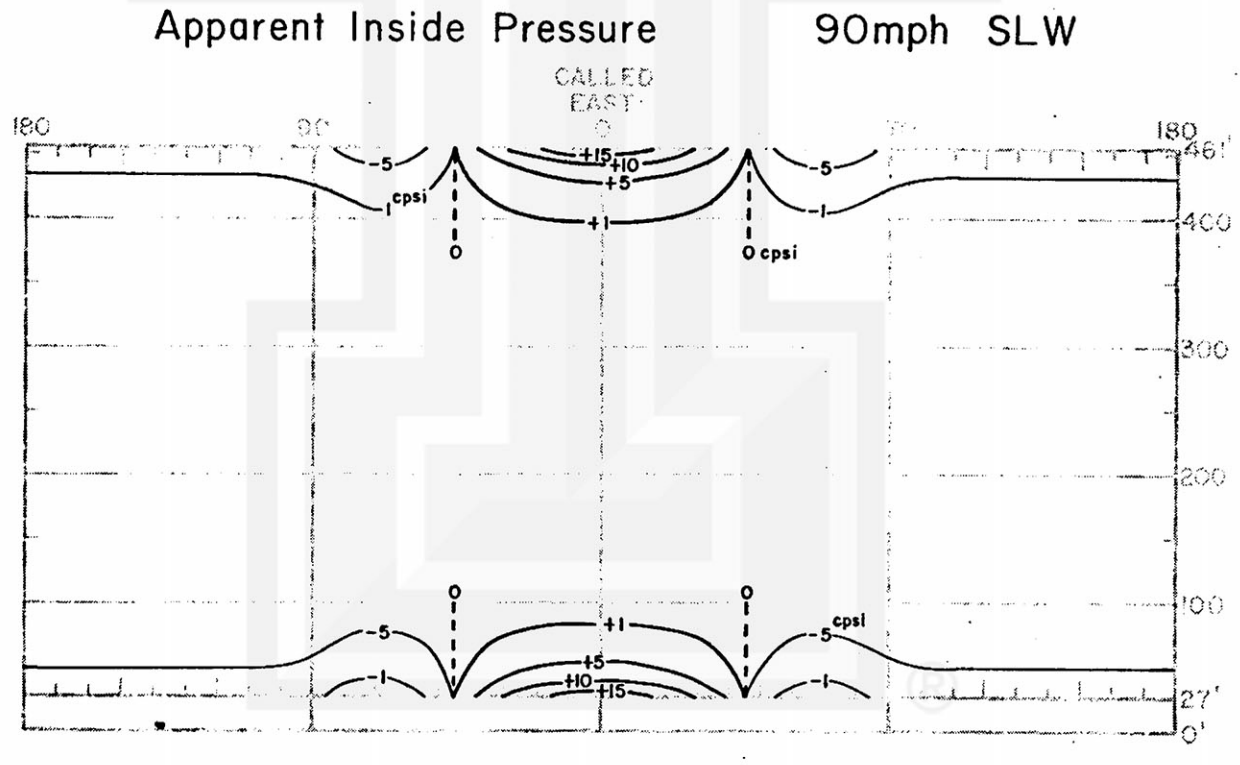

Figure 6. Apparent inside pressure induced by a 90 mph straight-line wind. The differential pressure can be computed as the difference between apparent outside pressure and apparent inside pressure.

3. PRESSURE DISTRIBUTION UNDER TORNADIC WIND

No measurments of pressure distribution around the cooling tower under tornadic wind are available at the present time. Making use of the pressure distribution discussed in the previous section, however, it is feasible to determine reasonable pressure distributions at the Grand Gulf cooling tower during the passage of the April 17, 1978 tornado.

The computation procedure used in this paper is as follows:

Step 1. Determine both β and V_β by intersecting the tornado wind field with the cooling tower from the ground to the top level (see Table 4 and Figure 7).

Step 2. Compute the field of stagnation pressure (see Figure 8).

Step 3. Compute pressure coefficients as a function of β only. The edge-effect function is not included (see Figure 9).

Step 4. Compute aerodynamic pressure, P_A , outside the shell from Eq. (1) and Steps 2 and 3 (see Figure 10).

Step 5. Compute vortex pressure, P_v , by intersecting the tornado vortex field with the cooling tower (see Table 5 and Figure 11).

Step 6. Compute static pressure, P_s , outside the shell by adding P_A in Step 4 and P_v in Step 5 (see Figure 12).

Step 7. Compute mean inside pressure, $\overline{P}_{in}$, from Eq. (2) by adding the static pressure along the top- and the base-edges of the tower.

Step 8. Compute apparent outside pressure, P'_{out} , by subtracting $\overline{P}_{in}$ in Step 7 from P_s in Step 6 (see Figure 13 in Section 5).

Step 9. Compute apparent inside pressure, P'_{in} , which is the product of P'_{out} in Step 8 and the edge-effect function of Eq. (5) and Table 3 (see Figure 14 in Section 5).

Step 10. Compute differential pressure, ΔP, in Eq. (10) by subtracting the apparent inside pressure in Step 9 from the apparent outside pressure in Step 8 (to be performed by other participants).

It has been agreed that Fujita will complete ten (10) charts showing the pressure distribution in Steps 8 and 9 at -4 seconds, -2 seconds, 0 second, +2 seconds, and +4 seconds. Step 10 and interpolations are to be performed by other participants.

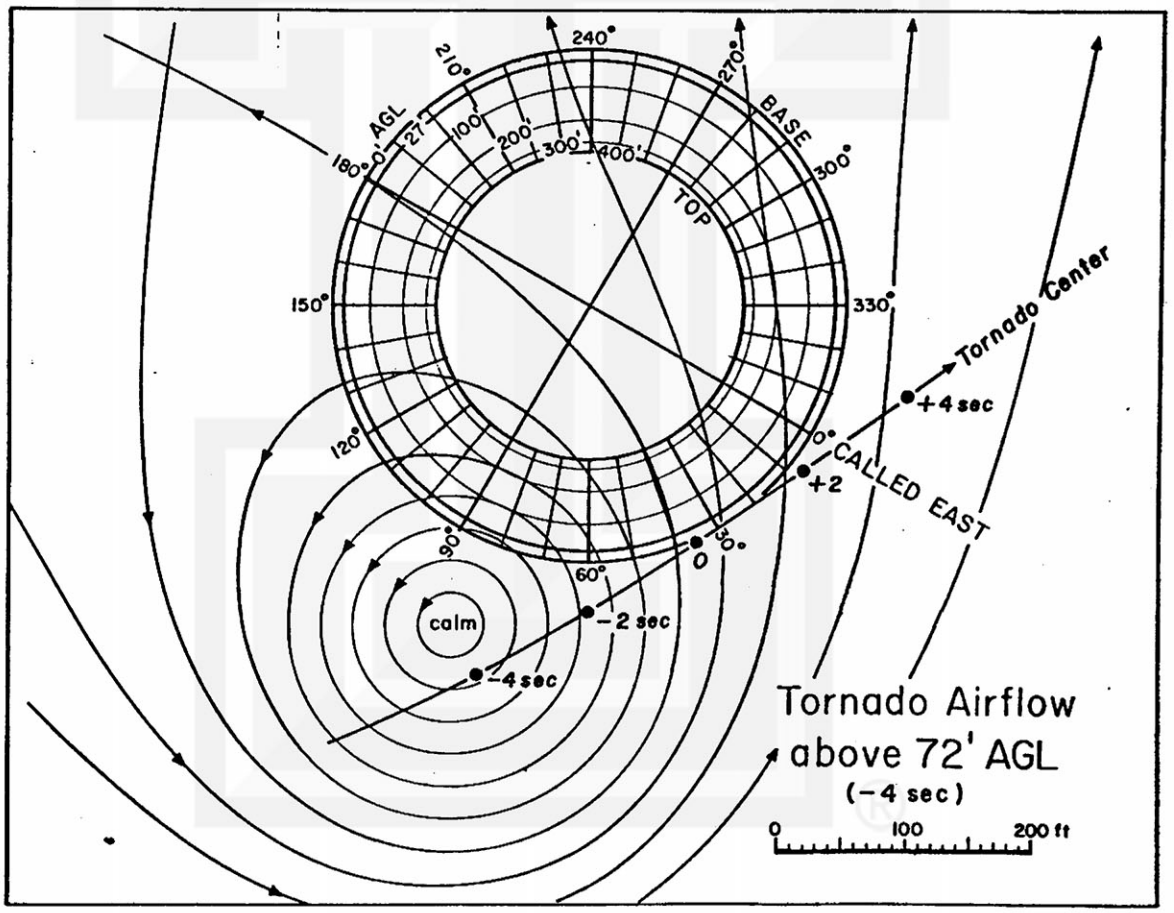

Figure 7. Intersections of tornado airflow at levels above 72-ft AGL and the cooling tower depicted by 0', 27', 100', 200', 300', and 400' radii. Undisturbed flow angles are computed as the angles of intersection between flow-lines and the tower circumferences at various AGL heights.

Table 4. Horizontal velocity, S of the air swirling around the tornado center.

Radii	Height in ft AGL		
R	72 ft (h=1.00)	27 ft (h=0.38)	15 ft (h=0.21)
0 ft	0 mph	0 mph	0 mph
50	40	34	31
100	80	85	81
150	120	118	111
200	90	102	100
250	72	82	80
300	60	68	66
400	45	51	51
500	36	40	40
600	30	33	34

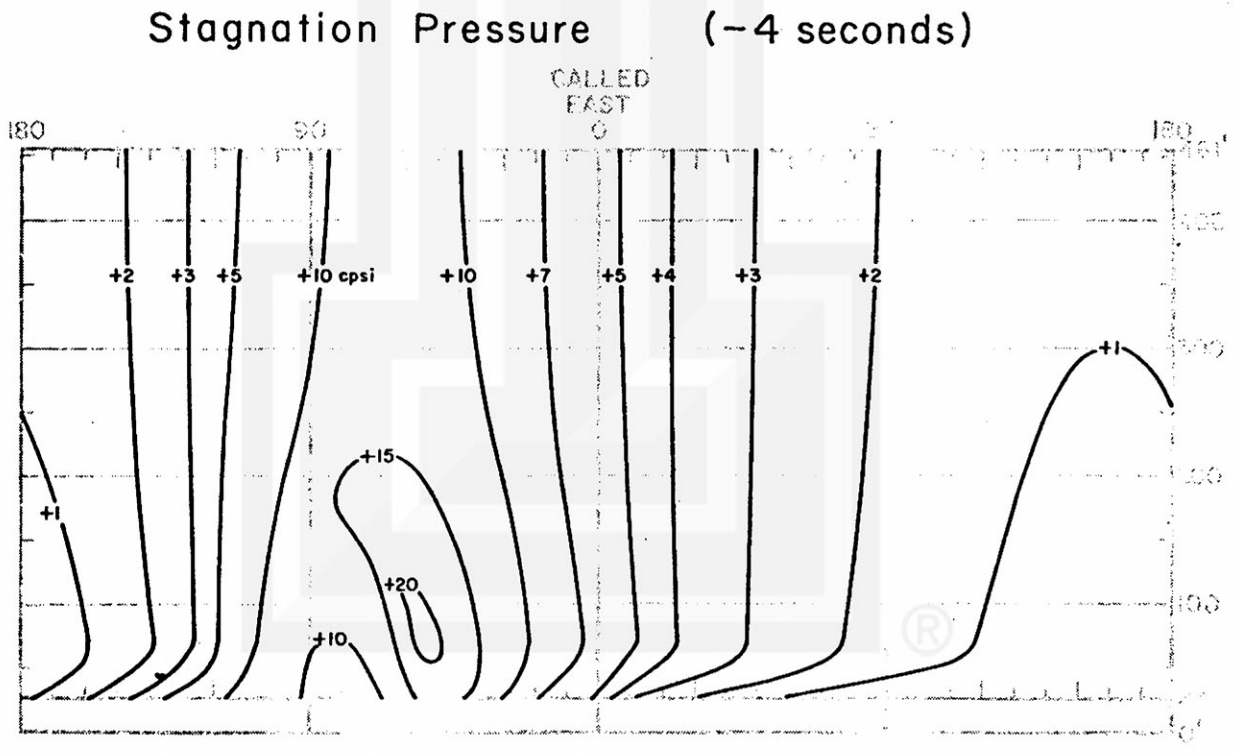

Figure 8. Stagnation pressure at -4 seconds (Step 2).

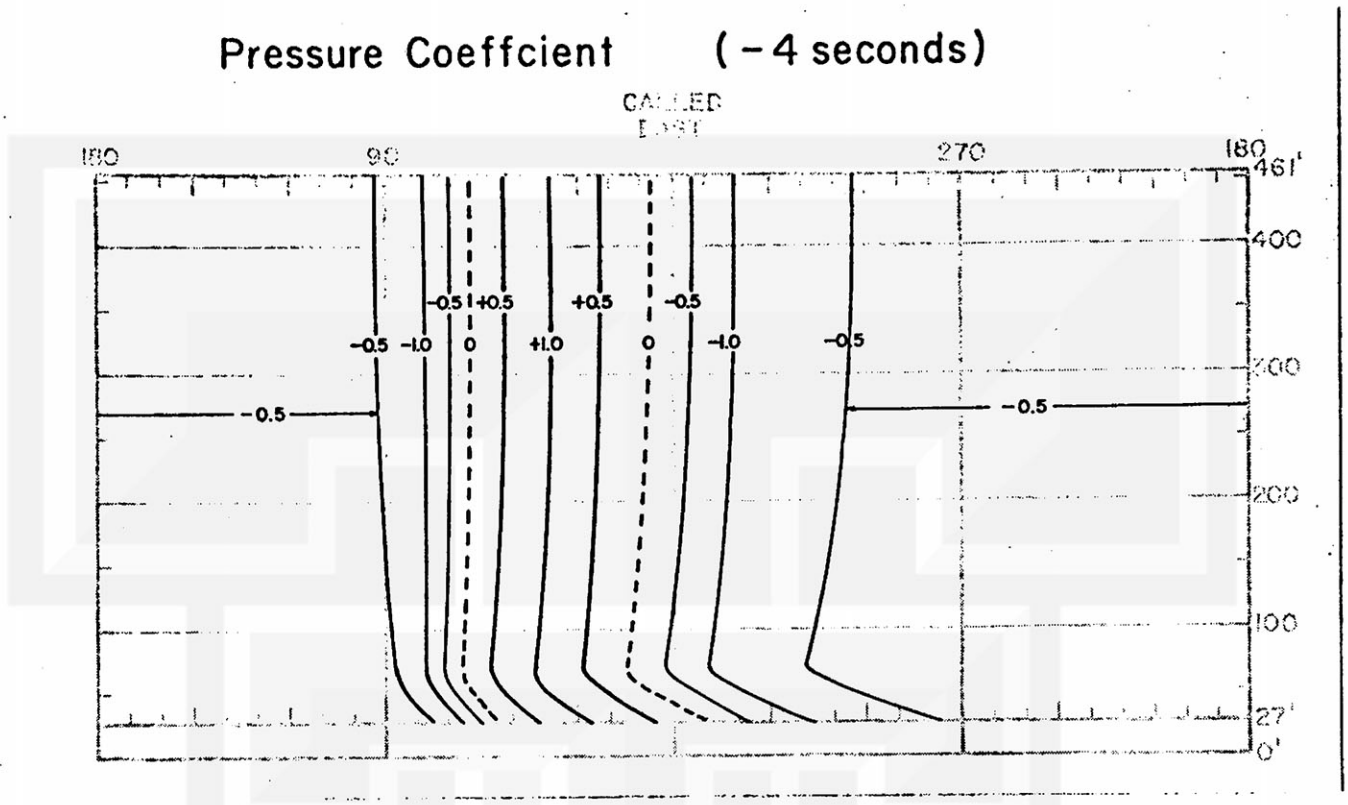

Figure 9. Pressure coefficient at -4 seconds (Step 3).

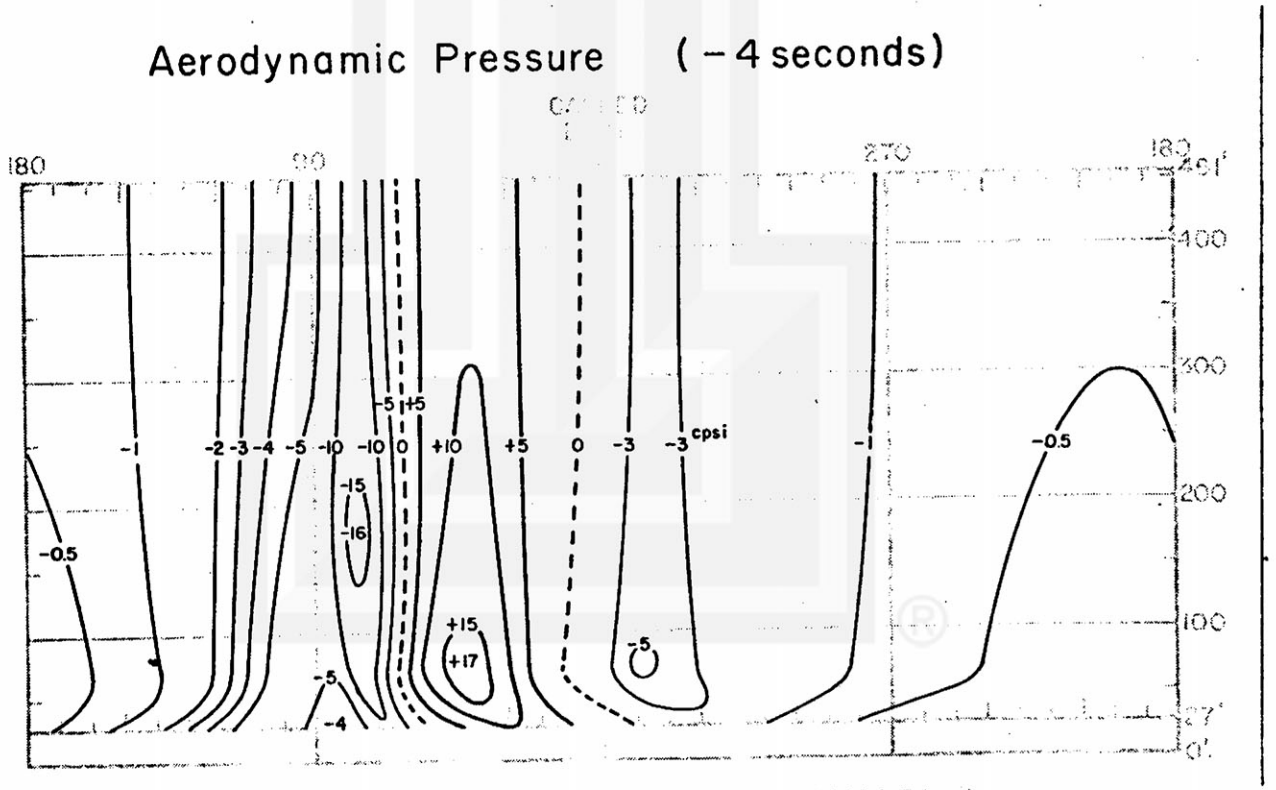

Figure 10. Aerodynamic pressure at -4 seconds (Step 4).

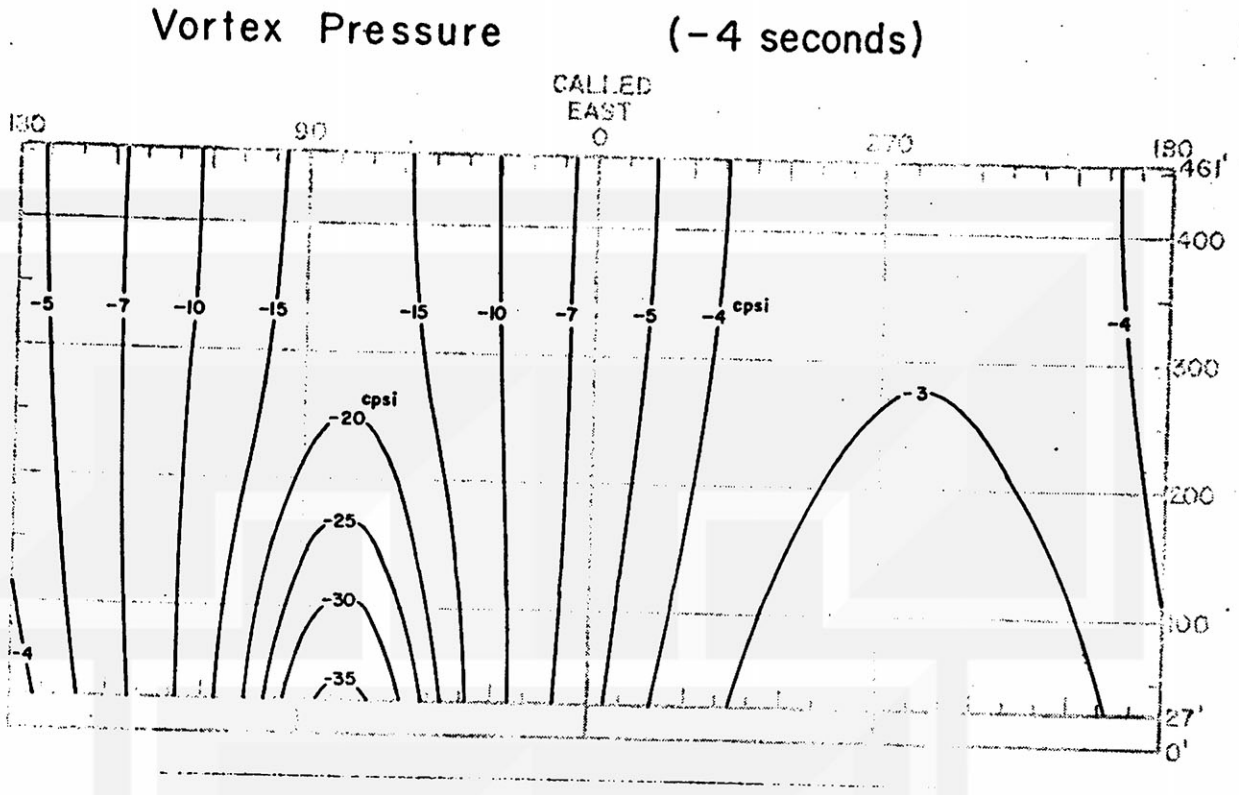

Figure 11. Vortex pressure at -4 seconds (Step 5).

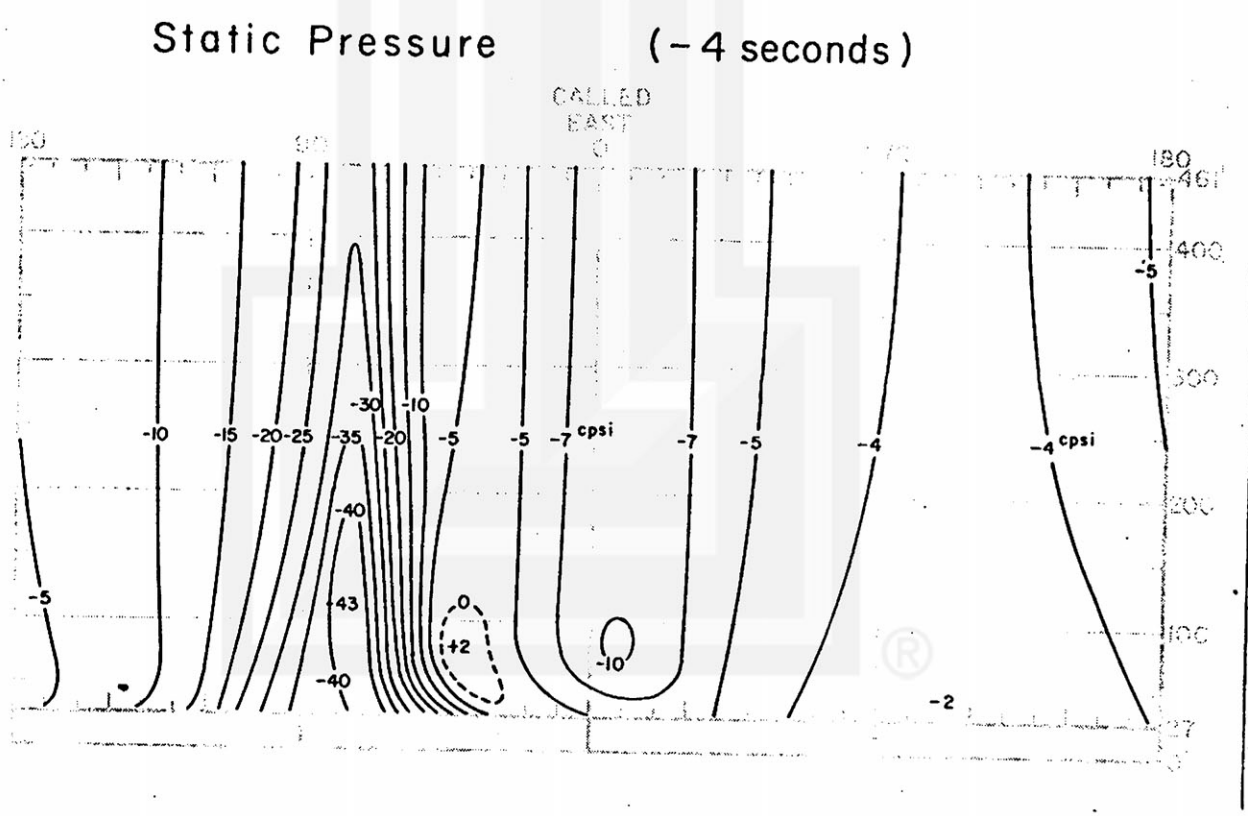

Figure 12. Staticpressure at -4 seconds (Step 6).

Table 5. Radius of tornado, R in ft at which the vortex pressure, P_v in cpsi occur. Input data are V_m = 120 mph, $\rho = 1.2 \times 10^{-3}$ g/cm^3.

P_v	R	P_v	R	P_v	R
0 cpsi	inf.	-10 cpsi	237 ft	-43 cpsi	79 ft
-1	750 ft	-15	194	-45	67
-2	530	-20	168	-46	60
-3	433	-25	150	-47	52
-4	375	-30	134	-48	42
-5	335	-35	116	-49	30
-7	283	-40	95	-50	0

4. WIND FIELD OF TORNADO

The structure and movement of the Grand Gulf tornado in relation to the cooling tower is extremely important in assessing the wind effect.

Since the technical report "Tornado Damage at the Grand Gulf, Mississippi Nuclear Power Plant Site: Aerial and Ground Surveys" by Fujita and McDonald (U.S. Nuclear Regulatory Commission, NUREG/CR-0383) does not include the technical data required for this analysis, Fujita completed Task A which is to be written as PART I of his report to Raths, Raths & Johnson, Inc. at a later date.

A summary of the tornado parameters obtained through Task A is:

Radius of outer core, R_o = 150 ft
Radius of inner core, R_n = 51 ft
Top of inflow height, H_i = 72 ft AGL
Translational velocity, T = 34 mph
Maximum tangential velocity, V_m = 120 mph

These parameters are used as input data to the tornado model, DBT-77 (Design-Basis Tornado completed in 1977) described in the "Workbook of Tornadoes and High Winds" by Fujita (SMRP Research Paper 165, September, 1978).

In computing the three-dimensional airflow, it was assumed that the tornado vortex above the top of the inflow height, H_i = 72 ft is constant with height all the way to the top of the tower. Because the tornado windspeed in the DBT-77 decreases gradually with the height above H_i, this assumption will give conservative estimates of wind effect. In view of the uncertainties in estimating the exact flow and pressure field, this conservative assumption should be regarded as realistic.

The horizontal velocity, S, of the air which swirled around the tornado center at R_o = 150 ft radius is shown in Table 4. 27 ft AGL is the height of the tower-shell base and 15 ft AGL, the mean representative height of the opening below the shell base. It should be noted that

$$S = (U^2 + V^2)^{\frac{1}{2}} \tag{13}$$

include both U, the radial velocity and V, the tangential velocity.

These velocities at the heights of the tower-base opening are given in Table 6. The mean horizontal velocity between the ground and 27 ft computed from Table 6 is 97.4 mph. Thus we write

$$\bar{S} = 0.87 \times S \text{ at } 15 \text{ ft} \tag{14}$$

This means that the mean flow speed below 27 ft AGL is 0.87 times the horizontal flow speed at the 15 ft AGL.

Table 6. Tangential, radial, and horizontal velocities at R_o, the radius of outer core tabulated as a function of the AGL height.

Height		Velocities		
H	h	V, tangential	U, radial	S, horizontal
27 ft	0.38	102 mph	59 mph	118 mph
24	0.33	100	61	117
21	0.29	98	62	116
18	0.25	95	62	113
15	0.21	93	63	112
12	0.17	89	62	108
9	0.13	85	61	105
6	0.08	79	58	98
3	0.04	70	52	87
0	0.00	0	0	0

The total inflow into the tower through the base opening is computed by

$$M_{base} = \Sigma \eta \, \bar{V}_n H_o \, \Delta C \tag{15}$$

where η denotes the efficiency of the inflow; $\bar{V}_n$, the mean normal velocity between 0 and 27 ft AGL; H_o , the height of the base opening; and ΔC, the 10° length at the base expressed by

$$\Delta C = 2\pi R_B / 36 \tag{16}$$

where R_B is the radius of the tower base.

$\bar{V}_n$ can be expressed by the normal velocity at the 15 ft AGL by using Eq. (14). Thus we write

$$M_{base} = \frac{1}{18} \eta \pi R_B H_o \times 0.87 \Sigma V_{n(15')} \tag{17}$$

The total outflow from the tower top is written as

$$M_{top} = \pi R_T^2 W \tag{18}$$

where R_T is the radius of the tower top and W, the updraft velocity.

Now, we equate Eq. (15) with Eq. (18) to obtain

$$W = 0.048 \eta H_o \frac{R_B}{R_T^2} \Sigma V_{n(15')} \tag{19}$$

where $V_{n(15')}$ must be obtained by determining both β and V_β at 15-ft level for every 10-degree azimuth all around the tower base.

Table 7 shows these values computed at -4 sec, -2 sec, 0 sec, +2 sec, and +4 sec. The total values at the end of this table are all positive, revealing that W is positive with a maximum at 0 second.

Using the constants, H_o = 27 ft, R_B = 197 ft, and R_T = 120 ft, the updraft in Eq. (19) can be reduced into

$$W = 0.018 \, \eta \Sigma V_{n(15')} \tag{20}$$

Table 7 now permits us to compute the updraft speeds at 5 different times. Results in Table 8 show that the maximum updraft speed occurring at time 0 second with 100% inflow efficiency was 16 mph, which is small enough to assume a uniform pressure distribution inside the tower except near the top and base edges.

Table 7. Undisturbed flow angle, β and flow speed, V_β in mph and its component velocity, V_n in mph normal to the tower circumference. + denotes the inflow component and -, the outflow. Values are computed at the 15 ft AGL.

Azimuths (called east)	-4 seconds			-2 seconds			0 second			+2 seconds			+4 seconds		
	V_β	β	V_n	V_β	β	V_n	V_β	β	V_n	V_β	β	V_n	V_β	β	V_n
0°	49	17°	+47	79	0°	+79	81	0°	+81	20	60°	+10	70	180°	-70
10	58	6	+58	87	-11	+85	64	10	+63	22	123	-12	104	160	-98
20	68	-7	+67	97	-14	+94	41	25	+37	39	148	-33	121	140	-93
30	80	-17	+77	82	-20	+77	30	53	+18	75	135	-53	120	130	-77
40	88	31	+75	61	-20	+57	25	97	-3	57	126	-34	106	117	-48
50	95	48	+64	37	-15	+36	37	130	-19	123	118	-58	95	108	-29
60	80	65	+34	15	-17	+14	75	125	-43	114	124	-64	84	100	-15
70	62	90	+1	12	-157	-11	103	122	-55	102	114	-41	76	92	-3
80	57	120	-29	57	160	-54	114	113	-45	93	97	-11	70	84	+7
90°	67	151	-59	82	140	-63	105	106	-29	82	87	+4	67	76	+16
100	82	175	-82	100	122	-53	93	97	-11	73	80	+13	64	68	+24
110	83	160	-78	90	112	-34	81	90	+1	67	75	+17	61	57	+33
120	75	140	-57	80	98	-11	71	80	+12	63	71	+21	57	53	+34
130	63	136	-45	70	92	-2	63	70	+22	58	60	+29	55	45	+39
140	51	111	-18	57	84	+6	56	63	+25	54	52	+33	53	43	+39
150	42	100	-7	47	74	+13	50	49	+33	50	41	+38	49	32	+42
160	36	97	-4	43	72	+13	45	43	+33	46	34	+38	46	19	+43
170	30	88	+1	37	65	+16	41	37	+33	43	23	+40	44	8	+44
180°	27	85	+2	33	63	+15	36	32	+31	40	19	+38	43	3	+43
190	25	85	+2	29	41	+22	33	27	+29	37	10	+36	40	2	+40
200	23	80	+4	27	42	+20	30	24	+27	35	7	+35	38	-8	+38
210	21	78	+4	25	45	+18	27	20	+25	33	5	+33	37	-15	+36
220	19	72	+6	24	40	+18	26	20	+24	32	3	+32	36	-16	+35
230	18	72	+6	23	43	+17	26	26	+23	31	5	+31	36	-17	+34
240	17	65	+7	22	47	+15	26	25	+24	31	-2	+31	38	-22	+35
250	17	67	+7	22	53	+13	27	16	+26	32	-4	+32	40	-24	+37
260	17	67	+7	23	50	+15	29	17	+28	35	0	+35	43	-33	+36
270°	18	70	+6	24	50	+15	30	20	+28	39	-2	+39	48	-31	+41
280	20	75	+5	26	45	+18	34	14	+33	45	-9	+44	57	-30	+49
290	22	76	+5	29	39	+23	38	12	+37	53	-10	+52	67	-32	+57
300	25	70	+9	33	38	+26	44	12	+43	63	-12	+62	79	-42	+59
310	27	58	+14	37	30	+32	50	10	+49	75	-14	+73	87	-55	+50
320	31	46	+22	41	30	+36	62	8	+61	85	-16	+82	70	-58	+37
330	35	37	+28	47	26	+42	73	8	+72	78	-15	+75	50	-70	+17
340	39	32	+33	56	20	+53	84	0	+84	59	-11	+58	30	-120	-15
350	44	21	+41	66	11	+65	93	-7	+92	36	20	+34	40	-160	-38
Total			+253 mph			+725 mph			+889 mph			+759 mph			+479 mph

Table 8. Updraft speeds computed from Eq.(19) assuming inflow efficiencies ranging between 70 and 100%.

Inflow efficiency	T I M E -4 sec	-2 sec	0 sec	+2 sec	+4 sec
100 %	4.5 mph	13.1 mph	16.0 mph	13.7 mph	8.6 mph
90 %	4.1	11.7	14.4	12.3	7.8
80 %	3.6	10.4	12.8	10.9	6.9
70 %	3.2	9.1	11.2	9.6	6.6
ΣV_n (mph)	+253	+725	+889	+759	+479

5. OUTSIDE AND INSIDE PRESSURES AT -4, -2, 0, +2, and +4 SECONDS

The final products of Task B defined in the minutes of the meeting on January 4, 1979, are ten (10) pressure-distribution charts at 5 different times. Two charts are provided for each analysis time, separated by two seconds. These two charts, as a pair, show the pressure distribution within the 360° azimuth (from called east) from the base to the top of the tower.

These charts are labeled as "Apparent Outside Pressure", P'_{out} and "Apparent Inside Pressure", P'_{in} . The differential pressure in Eqs. (6) and (7) can be computed from

$$\Delta P = P_{out} - P_{in} \qquad (6)$$

$$= P'_{out} - P'_{in} \qquad \text{same as (7)}$$

For the purpose of computing the differential pressure, the term "Apparent" may be dropped.

The list of final products included in this report is:

Apparent Outside Pressure at -4 seconds (Figure 13)
Apparent Inside Pressure at -4 seconds (Figure 14)

Apparent Outside Pressure at -2 seconds (Figure 15)
Apparent Inside Pressure at -2 seconds (Figure 16)

Apparent Outside Pressure at 0 second (Figure 17)
Apparent Inside Pressure at 0 second (Figure 18)

Apparent Outside Pressure at +2 seconds (Figure 19)
Apparent Inside Pressure at +2 seconds (Figure 20)

Apparent Outside Pressure at +4 seconds (Figure 21)
Apparent Inside Pressure at +4 seconds (Figure 22)

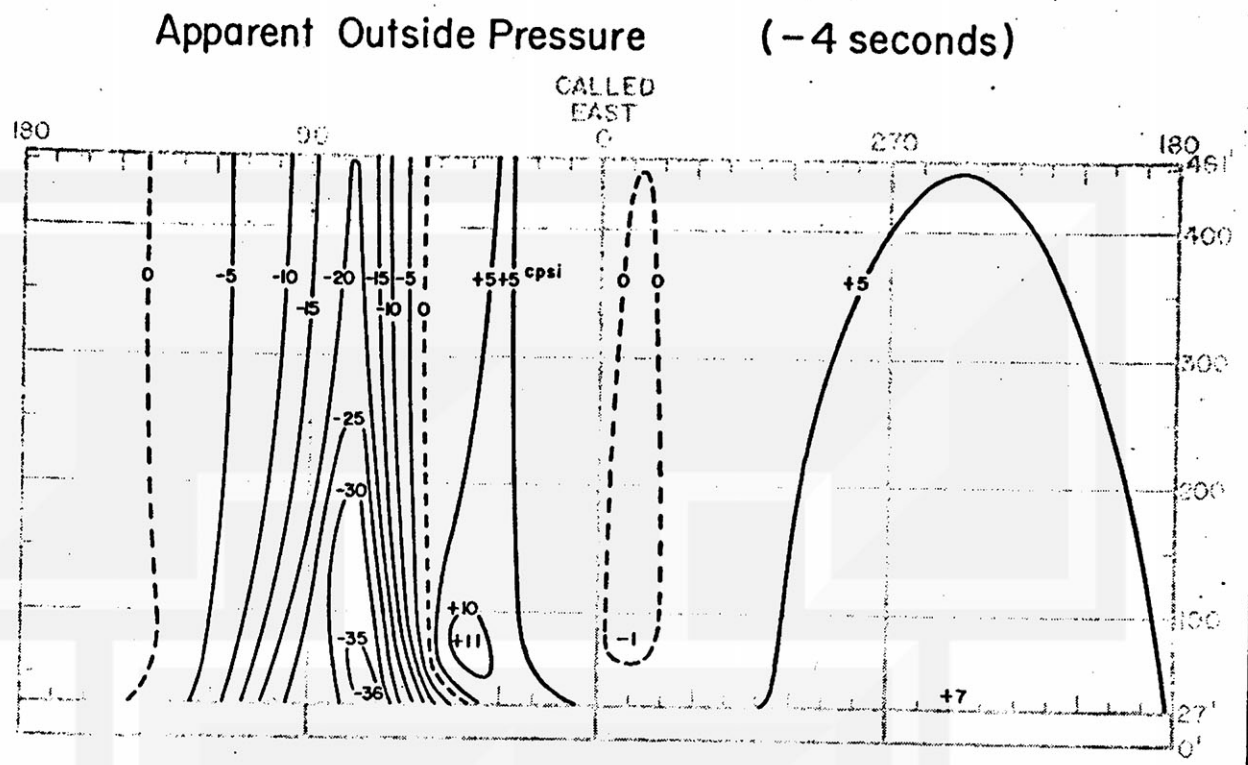

Figure 13. Apparent outside pressure at -4 seconds (Step 8).

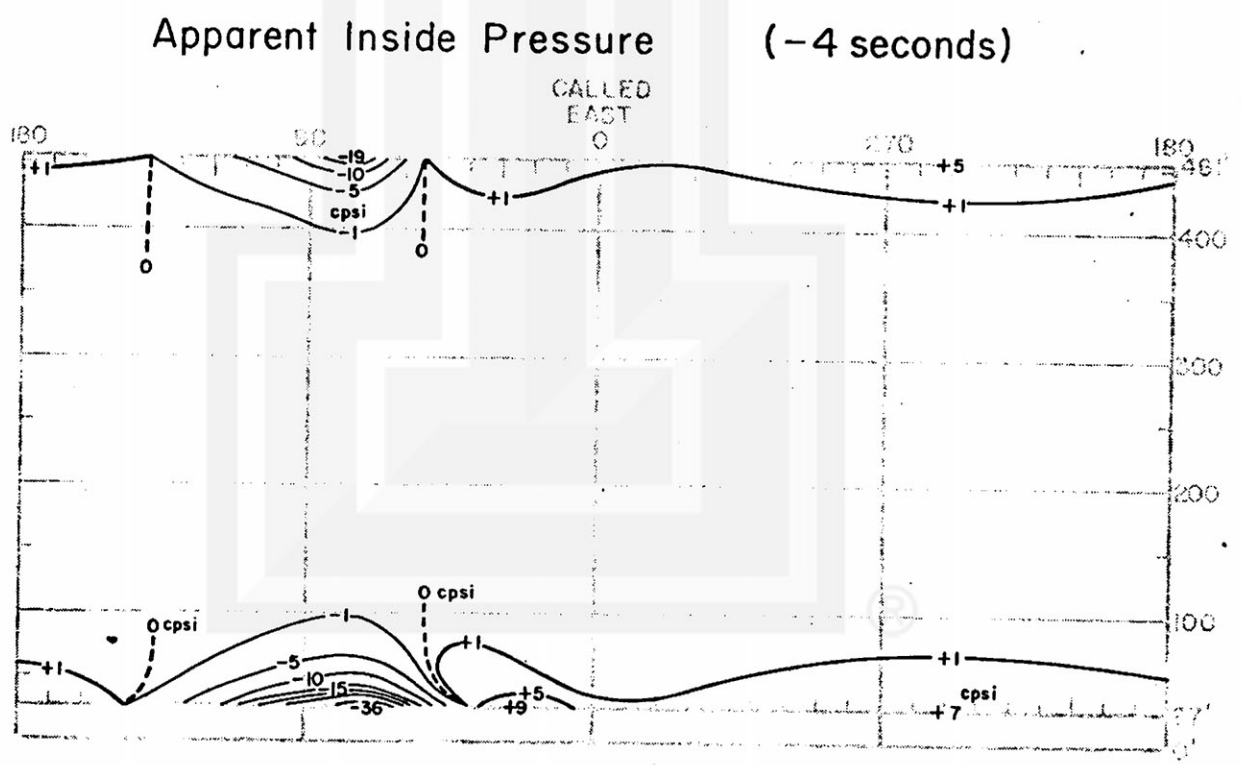

Figure 14. Apparent inside pressure at -4 seconds (Step 9).

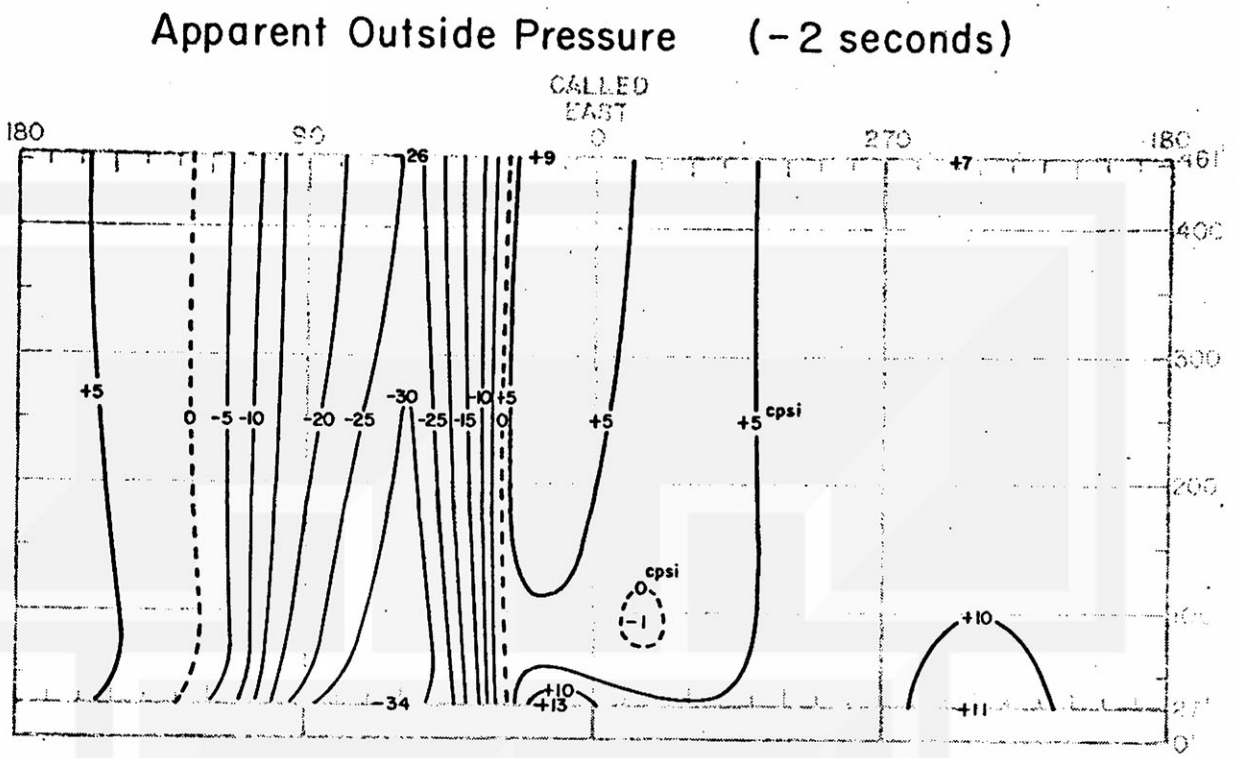

Figure 15. Apparent outside pressure at -2 seconds.

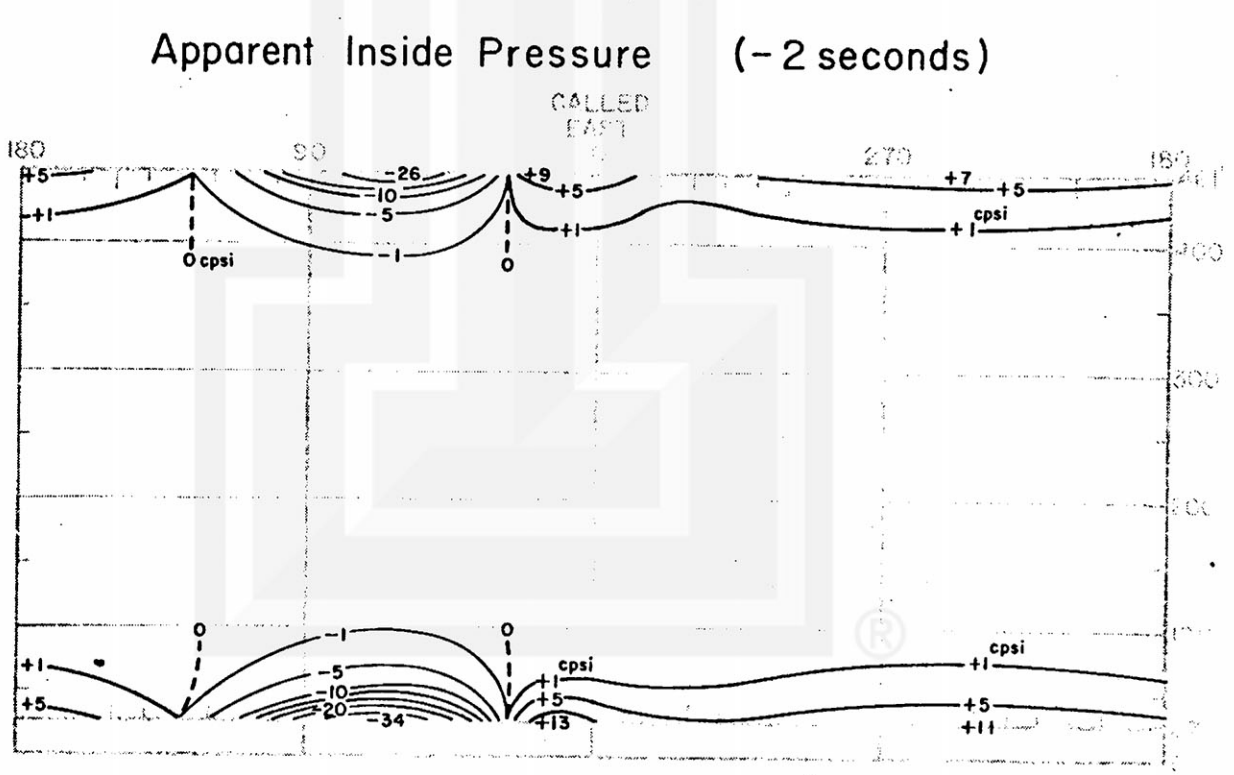

Figure 16. Apparent inside pressure at -2 seconds.

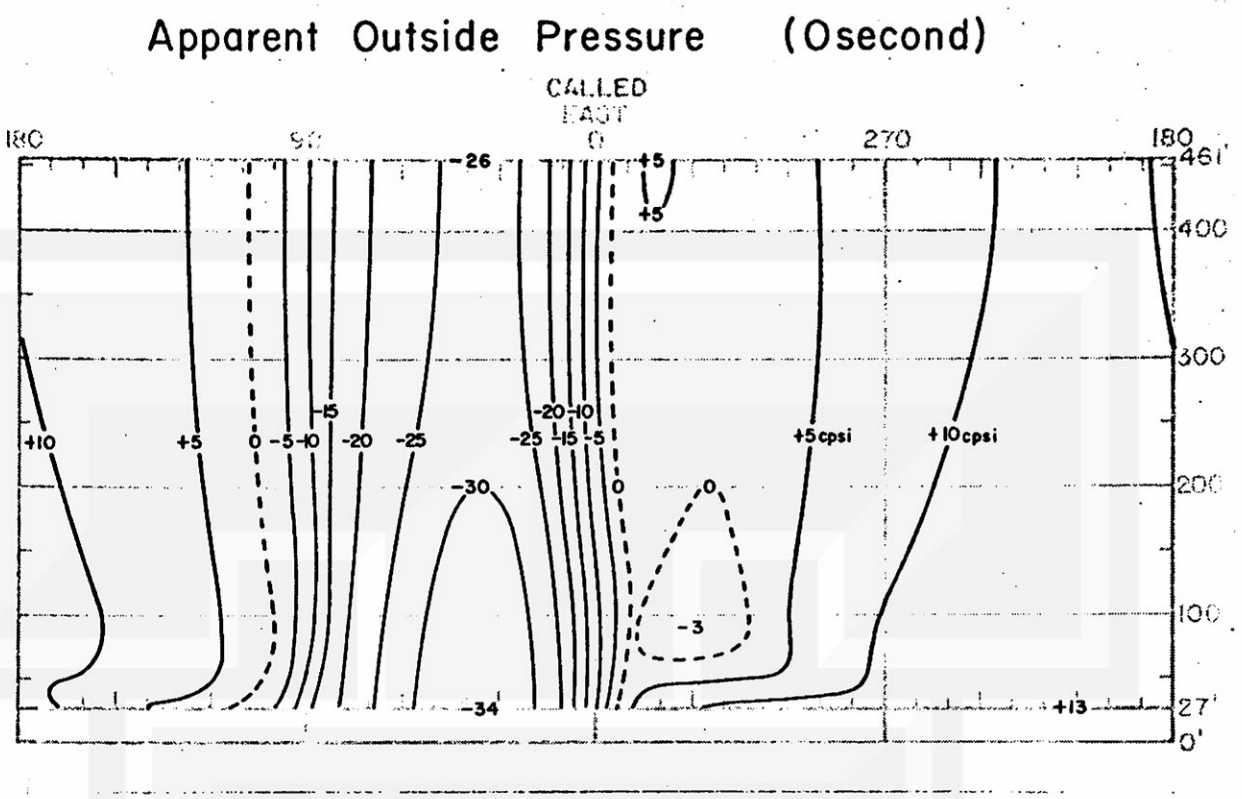

Figure 17. Apparent outside pressure at 0 second.

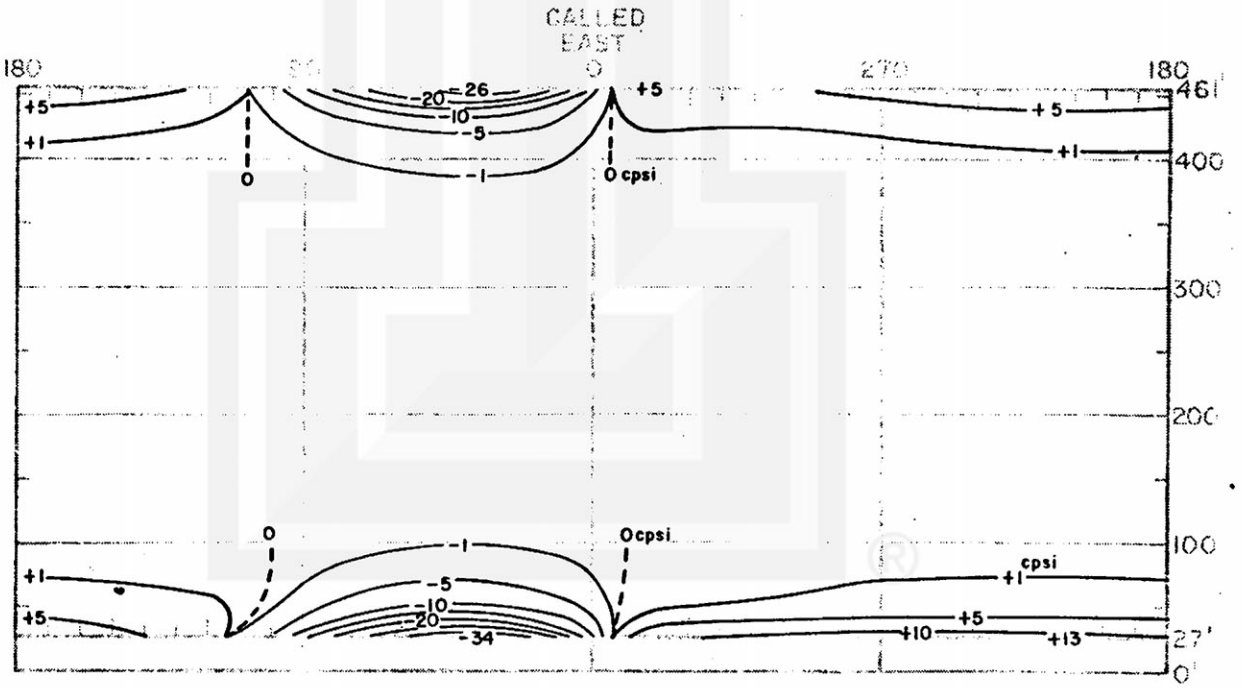

Figure 18. Apparent inside pressure at 0 second.

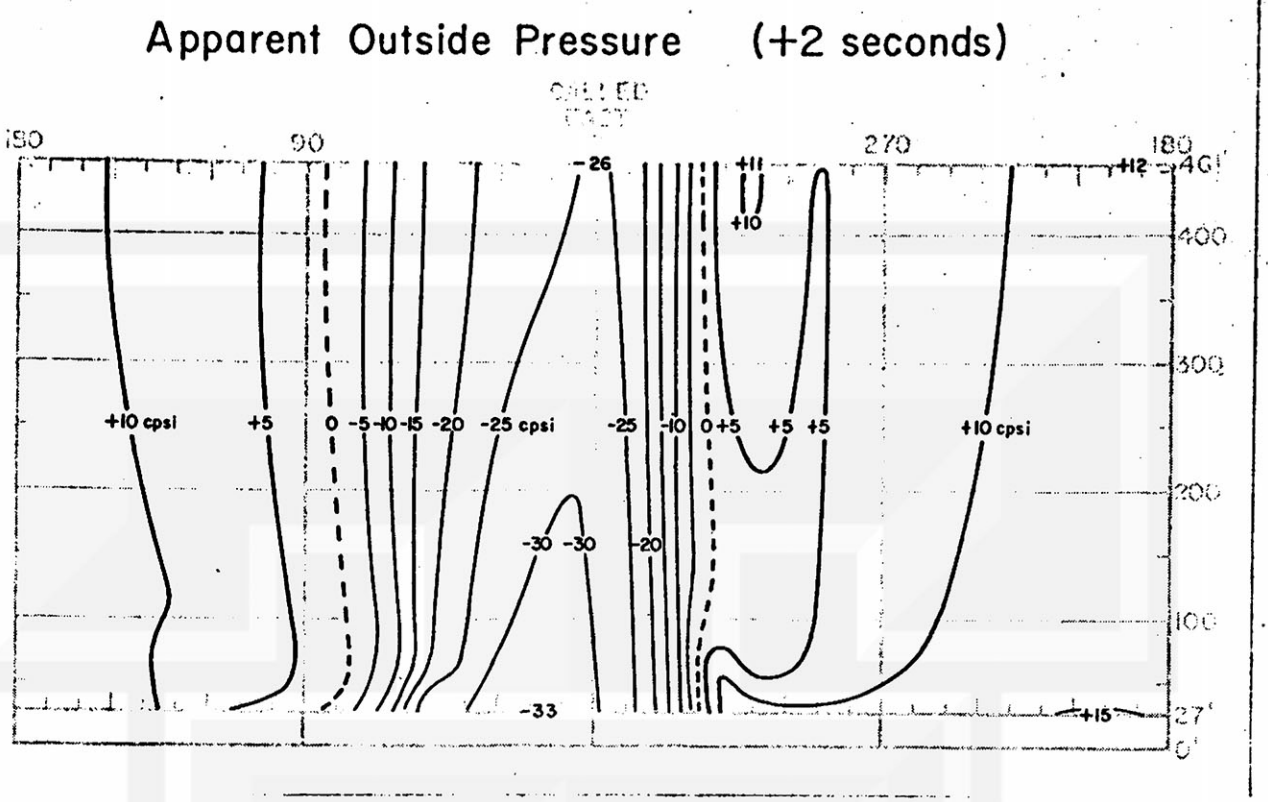

Figure 19. Apparent outside pressure at +2 seconds.

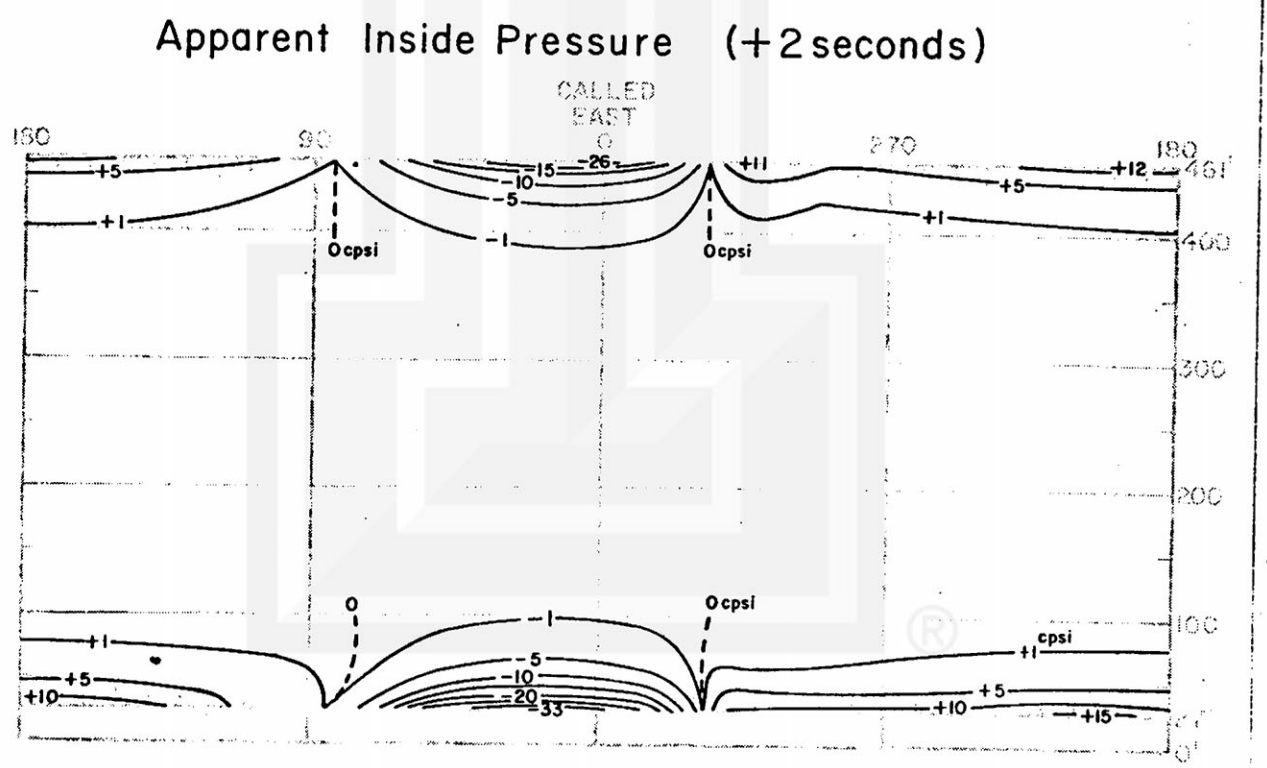

Figure 20. Apparent inside pressure at +2 seconds.

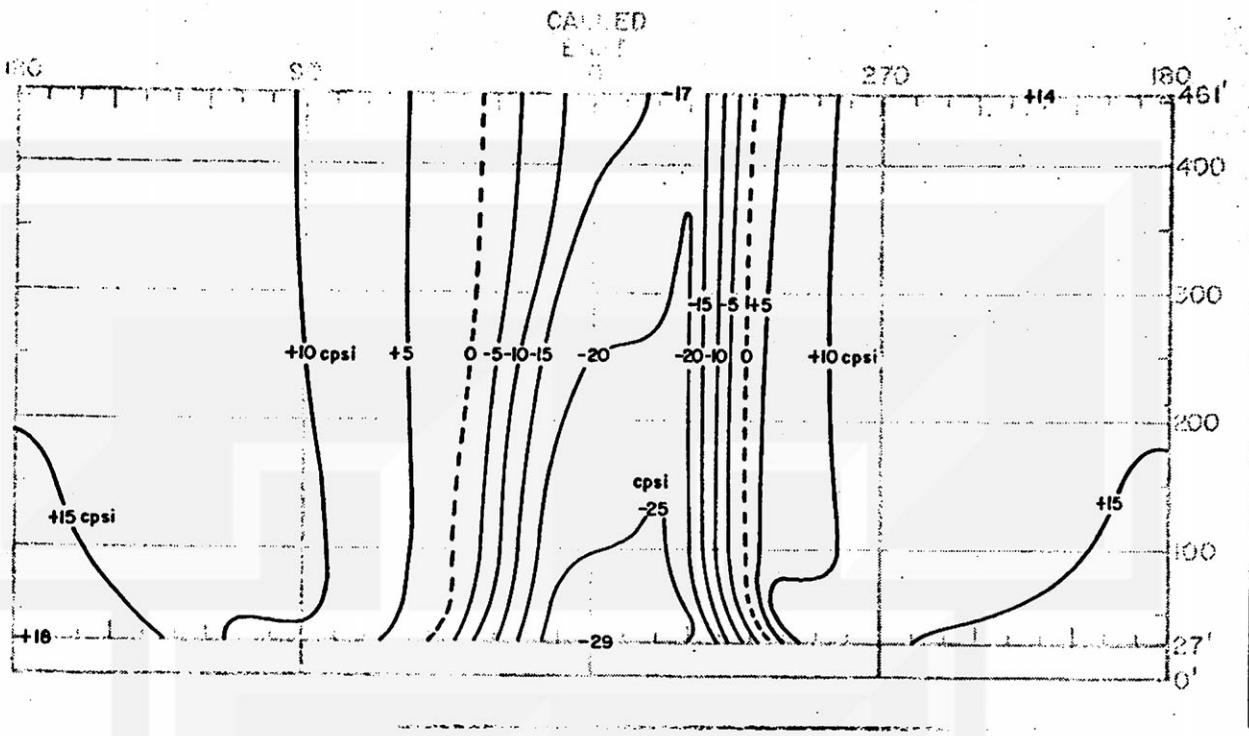

Figure 21. Apparent outside pressure at +4 seconds.

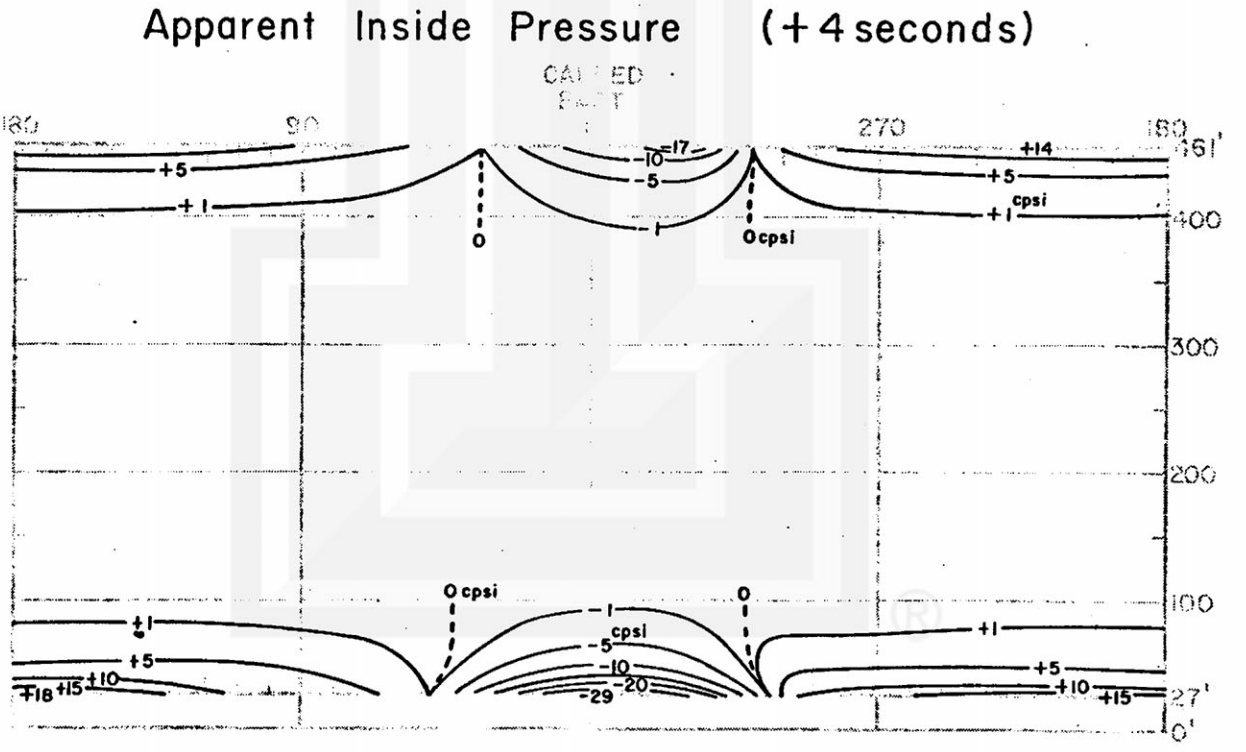

Figure 22. Apparent inside pressure at +4 seconds.

-- Acknowledgements --

Research Tasks presented in this report have been sponsored by Raths, Raths & Johnson, Inc. under agreement with Mr. Guedelhofer on December 22, 1978 and authorization by Mr. Raths dated January 15, 1979.

Authorized users of this report may call T. Theodore Fujita whenever necessary.

Home (312) 288-3045 at 5727 S. Maryland Avenue
Chicago, IL 60637 or

Office (312) 753-8114 at The University of Chicago
5734 S. Ellis Avenue
Chicago, IL 60637.

[redacted]